

## Electron Density in Potassium Tetrachloropalladate ( $K_2PdCl_4$ ) from Synchrotron Radiation Data

BY J. R. HESTER, E. N. MASLEN AND N. SPADACCINI

*Crystallography Centre, University of Western Australia, Nedlands 6009, Australia*

N. ISHIZAWA

*Research Laboratory of Engineering Materials, Tokyo Institute of Technology, 4259 Nagatsuta, Midori-Ku, Yokohama 227, Japan*

AND Y. SATOW

*Faculty of Pharmaceutical Sciences, University of Tokyo, Hongo 7-3-1, Bunkyo-ku, Tokyo 113, Japan*

(Received 1 December 1992; accepted 10 May 1993)

### Abstract

The difference electron density has been evaluated for potassium tetrachloropalladate,  $K_2PdCl_4$ , using synchrotron radiation at 0.7 and 0.9 Å at room temperature. A similar data set was measured with Mo  $K\alpha$  radiation. The  $\Delta\rho$  maps for the synchrotron data sets are consistent, and agree approximately with the Mo  $K\alpha$  map away from the Pd nucleus. There is marked depletion of electrons near the Pd core, and substantial movement of electron density near the structural cavities. The Pd-atom charge is approximately +2, but the K-atom charge is significantly negative. These charges result from transfer of electron density from tightly packed to more open regions of the structure, and do not necessarily reflect atomic electronegativities.  $K_2PdCl_4$ ,  $P4/mmm$ ,  $Z = 1$ ,  $\mu_{0.7} = 4.1784$ ,  $\mu_{0.9} = 8.6075 \text{ mm}^{-1}$ ,  $F(000) = 152$ ,  $T = 293 \text{ K}$ ,  $M_r = 326.4$ ,  $a = 7.0750 (5)$ ,  $c = 4.1158 (5) \text{ \AA}$ ,  $V = 206.02 (4) \text{ \AA}^3$ ,  $D_x = 2.631 \text{ Mg m}^{-3}$ .

### Introduction

In principle X-ray diffraction measurements of one-electron densities should sharpen our understanding of the variation of the properties of atoms with their row number in the Periodic Table. This requires a set of crystalline compounds which contain the same atom in different valence states. These compounds should be sufficiently similar to permit meaningful comparison of their electron densities. These requirements are met by the halides of the alkali metals with the platinoid elements Ni, Pd and Pt in which the platinoid elements appear with +4 (*e.g.*  $K_2PdCl_6$ ) and +2 (*e.g.*  $K_2PdCl_4$ ) valence states. The feasibility of studying these compounds accurately by X-ray diffraction is shown in the analysis of the electron density in  $K_2PdCl_4$  using Mo  $K\alpha$  radiation by Takazawa, Ohba & Saito (1988).

Measurement of the electron density in structures containing heavy atoms requires very accurate diffraction data because the changes in the valence-electron density are small relative to the total density for such atoms. The secondary-extinction corrections in the data refinement of Takazawa, Ohba & Saito (1988) are large, but the expressions for those corrections were derived assuming that the effects of secondary extinction are small. We have emulated that study in order to reduce the effect of the extinction treatment on the refined parameters and the difference electron density.

Small crystals were selected for study in order to lower secondary extinction to a level such that perturbation treatments of the corresponding corrections should be reliable. The use of those small crystals results in a concomitant reduction in the scattering power of the crystal, which could jeopardize the statistical precision of the weaker structure factors if these were measured with low-flux X-ray tube sources. We therefore studied the crystals using synchrotron radiation which, because of its high flux, alleviates the difficulty.

Maslen & Spadaccini (1993) show how unbiased estimates of extinction can be obtained by minimizing differences between intensities of equivalent reflections with different path lengths. The tunability of synchrotron sources provides an additional measure of extinction, by permitting intensity ratios for data sets collected at different wavelengths to be compared.

### Experimental

Crystals, grown by mixing hot acidified aqueous solutions of  $PdCl_2$  and KCl in stoichiometric proportions, were rectangular prisms elongated along  $c$  and bounded by large {100} and small {101} faces. The

specimen selected for the synchrotron study had dimensions  $30 \times 70 \times 110 \mu\text{m}$ . The crystals were mounted with their long axis approximately at right angles to the  $\varphi$  axis of the goniometer in order to obtain a large spread in path length for equivalent reflections.

The synchrotron diffraction data were measured on the BL14A four-circle diffractometer facility at the Photon Factory. Beams with wavelength  $\lambda = 0.9000$  (1) and  $0.7000$  (1) Å were monochromated with an Si(111) crystal, using a curved mirror to concentrate the X-rays (Satow & Iitaka, 1989). Synchrotron lattice parameters were determined from six reflections with  $43 < \theta < 45^\circ$  (0.7 Å) and  $48 < \theta < 50^\circ$  (0.9 Å). The intensity data were corrected for dead-time counting losses. The true count rate  $R_L$  at each point in a reflection profile is expressed as the expansion

$$R_L = R_0[1 + C_1(R_0\tau) + C_2(R_0\tau)^2 + C_3(R_0\tau)^3 + \dots],$$

where  $R_0$  is the observed count rate and  $\tau$  is the counter dead-time. Values for  $\tau$  and the coefficients  $C_1$  and  $C_2$  in the series were determined by recording counts before and after inserting an absorber into the beam for a range of intensities. The value of  $\tau$  determined was 1.2  $\mu\text{s}$ . Corrections were negligible for count rates less than 20 000 counts  $\text{s}^{-1}$ . The corrections were reliable up to true count rates of 150 000 counts  $\text{s}^{-1}$ .

Analysis of the synchrotron data measured initially revealed that intensities for some strong reflections were outside the range for which dead-time corrections could be applied accurately. In order to avoid error because of the dead-time corrections, a small inner sphere of reflections containing all dead-time-affected reflections was re-collected at lower beam intensity. After absorption correction the program *SCALE1* (Alden, Freer & Stewart, 1990) was used to determine relative scales for the two data sets at each wavelength and all reflections were then combined.

The analysis of extinction corrections by the method of Maslen & Spadaccini (1993) indicated that there was no significant correlation between path length and  $F^2$ . The conclusion that the extinction corrections were not significant was confirmed by a lack of wavelength dependence in the intensities for the strong reflections. The  $\lambda^3$  dependence of the instantaneously reflected intensity would make  $|F_o| - |F_c|$  more strongly negative for extinction-affected reflections with  $\lambda = 0.9$  Å than with  $\lambda = 0.7$  Å. The lack of a consistent trend of this type confirmed that extinction did not affect the data significantly.

This contrasts with the large extinction correction applied by Takazawa *et al.*, suggesting that the degree of crystallinity of the samples differs.

Mo  $K\alpha$  radiation from an X-ray tube was monochromated using the 002 reflection from an oriented graphite crystal in the equatorial setting. Mo  $K\alpha$  intensity data measured with a second crystal (dimensions  $40 \times 60 \times 160 \mu\text{m}$ ) also showed no extinction effect.

Variances in measured structure factors  $\sigma^2(F_o)$  from counting statistics, were modified for source instability using the program *DIFDAT* and increased when necessary by applying the Fisher test option of the program *SORTRF* (Hall & Stewart, 1990) when comparing intensities of equivalent reflections. Full-matrix least-squares refinement weights  $w = 1/\sigma^2(F_o)$  for all independent reflections, *i.e.* following good statistical practice, no reflections were classified arbitrarily as 'unobserved'. Atomic scattering factors of Cromer & Mann (1968) with the anomalous-dispersion corrections of Cromer & Liberman (1970), interpolated to give  $\Delta f'$  and  $\Delta f''$  values of 0.244, 0.437 for K,  $-0.724$ , 1.679 for Pd and 0.199, 0.284 for Cl at 0.9 Å, and 0.199, 0.241 for K,  $-0.993$ , 0.974 for Pd and 0.147, 0.153 for Cl at 0.7 Å.  $F_c$  was calculated using neutral spherically symmetric free atoms located at the atomic positions. No multipole parameters were refined. Further refinement details are given in Table 1.\* The computer programs *STARTX*, *DIFDAT*, *ABSORB*, *ADDDATM*, *ADDREF*, *FC*, *CRYLSQ*, *BONDLA*, *FOURR*, *CHARGE*, *CONTRS*, *SLANT* and *PLOT* from the *Xtal3.0* system of crystallographic programs (Hall & Stewart, 1990), installed on Sun workstation computers, were used in the analysis.

### Structural parameters

With the Pd atom at the cell origin, the Cl atom is at  $x, x, 0$ , and the K atom is  $0, \frac{1}{2}, \frac{1}{2}$ . The refined values for the  $x$  coordinate and the thermal parameters are compared in Table 2 with the corresponding values obtained by Takazawa, Ohba & Saito (1988). The  $x$  coordinate agrees for all data sets. The vibrational parameters indicate that the Pd atom is packed more tightly than the K and Cl atoms in the structure, being confined more strongly in the (001) planes containing the four Pd—Cl bonds than along the Pd—Pd contact in the [001] direction. There is a modest difference between the  $U_{11}$  parameters for Pd and Cl determined from the two sets of synchrotron radiation data.  $U_{11}$  for K differs markedly from that obtained by Takazawa, Ohba & Saito.

\* Lists of structure factors have been deposited with the British Library Document Supply Centre as Supplementary Publication No. SUP 71117 (11 pp.). Copies may be obtained through The Technical Editor, International Union of Crystallography, 5 Abbey Square, Chester CH1 2HU, England.

Table 1. *Experimental and refinement parameters*

	0.9 Å	0.7 Å	Mo K $\alpha$
Diffractometer	Rigaku	Rigaku	P2 <sub>1</sub>
Monochromator	Silicon	Silicon	Graphite
Scan type	$\theta$ - $2\theta$	$\theta$ - $2\theta$	$\theta$ - $2\theta$
$\theta$ -scan width (°)	0.90	0.72	1.7 + 0.35tan $\theta$
Maximum sin $\theta/\lambda$ (Å <sup>-1</sup> )	1.007	1.093	1.08
No. of reflections measured			8722
first data set	6728	8932	
second data set	726	726	
Instability factor	$2.8 \times 10^{-3}$	$1.9 \times 10^{-3}$	$2.7 \times 10^{-4}$
Transmission range in absorption correction	0.4919–0.7761	0.7110–0.8695	0.5715–0.8191
$R_{int}$	0.0334	0.0380	0.0308
No. of independent reflections ( $ F_{hkl}  \geq 0$ )	565	710	689
$R$	0.023	0.021	0.040
$wR$	0.020	0.020	0.026
$S$	5.239	3.96	2.5
$\Delta/\sigma_{max}$	$2.2 \times 10^{-4}$	$3.2 \times 10^{-5}$	$4.4 \times 10^{-2}$
$\Delta\rho_{max}$ (e Å <sup>-3</sup> )	0.8	0.8	1.2
$\Delta\rho_{min}$ (e Å <sup>-3</sup> )	-1.2	-1.3	-4.0

Table 2. *Vibrational parameters ( $U_{ij} \times 10^3 \text{ \AA}^2$ ) and  $x(\text{Cl})$* 

	0.9 Å	0.7 Å	Mo K $\alpha$	Takazawa, Ohba & Saito (1988)
<b>K</b>				
$U_{11}$	48.8 (3)	48.8 (2)	46.6 (6)	57.3 (2)
$U_{22}$	29.0 (2)	28.7 (2)	27.5 (4)	28.5 (1)
$U_{33}$	27.8 (1)	27.4 (1)	26.4 (4)	27.1 (1)
<b>Pd</b>				
$U_{11} = U_{22}$	20.30 (4)	19.96 (4)	17.8 (1)	18.86 (3)
$U_{33}$	23.92 (6)	23.92 (5)	22.3 (2)	22.96 (2)
<b>Cl</b>				
$U_{11} = U_{22}$	25.46 (7)	24.93 (7)	23.7 (2)	24.98 (2)
$U_{33}$	41.0 (2)	40.9 (1)	40.0 (3)	42.3 (1)
$U_{12}$	-2.96 (8)	-3.00 (7)	-2.8 (2)	-3.53 (5)
$x$	0.23076 (3)	0.23073 (3)	0.23081 (6)	0.23066 (2)

### Atomic charges

Atomic charges, determined by projecting  $\Delta\rho$  onto atomic density basis functions following the method of Hirshfeld (1977) are listed in Table 3. The charges on each atom for the three data sets are broadly consistent. The Pd atom is strongly depleted of electrons, and carries a charge in the range +2 to +3. Cl carries a small charge, having a negative sign consistent with its electronegativity. However, the K-atom charge of approximately -1 contrasts with its formal value of +1. Thus inter atom transfer of electron density correlates at best only weakly with electronegativity and formal charge. However, the electron movement can be readily understood in terms of the effect of the exchange interaction, which becomes strongly electron depleting when tight packing forces overlap between electrons with parallel spins. Electrons are transferred from the Pd atom, which is tightly packed, to those which have greater freedom of movement, which in this case is the K atom.

Although the broad trends for the charges listed in Table 3 are consistent, their numerical values do not agree as closely as expected if the standard deviations were a true measure of their reliability. The standard deviations in the charges, evaluated by the method of

Table 3. *Atomic charges (e)*

	0.9 Å	0.7 Å	Mo K $\alpha$
K	-1.118 (2)	-0.936 (6)	-0.76 (4)
Pd	2.878 (4)	1.894 (7)	1.92 (8)
Cl	-0.160 (2)	-0.006 (7)	-0.10 (4)

Davis & Maslen (1978) reflect the standard deviations in the measured structure factors. The significant discrepancies between the numerical values for the three data sets in Table 3 indicate that systematic errors in the measured structure factors, not allowed for in the standard deviations, reduce the accuracy of those charges. The 0.7 Å charges in Table 3 agree at least as well with the Mo K $\alpha$  values as they do with the 0.9 Å charges, although the reliability indices suggest that on the whole the Mo K $\alpha$  data are less accurate.

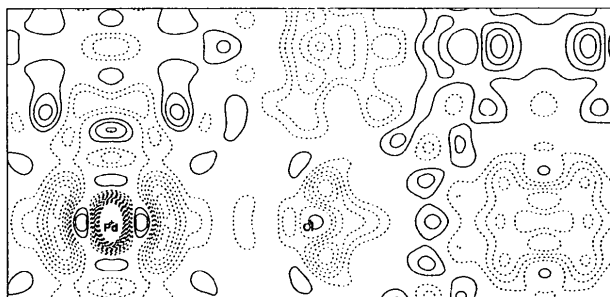
Atomic charges involve integrals, over large volumes compared with the resolution of the experiment, which are mainly determined by the low-angle structure factors. The anomalies in Table 3 are accounted for if it is assumed that the large low-angle structure factors contain systematic errors that are not accounted for by the standard deviations. The most probable source of the inaccuracy is the dead-time corrections. There is some uncertainty about the optimum choice of algebraic form for the correction, and the accuracy of the dead-time constant for the NaI scintillation counter is uncertain. The consequences of dead-time correction errors are more serious for the 0.9 Å data. For that reason the 0.7 Å charges, being favoured by the Mo K $\alpha$  experiment that is less affected by dead-time errors, should be preferred.

### Electron density

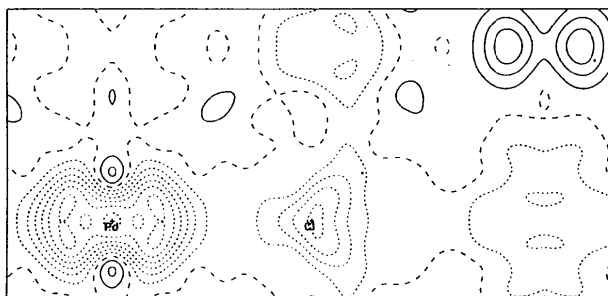
Difference electron densities in the (110) plane for K<sub>2</sub>PdCl<sub>4</sub> displayed in Figs. 1(a) and 1(b) are calculated from Mo K $\alpha$  and 0.7 Å data, respectively. The reduction in high-angle noise achieved by using synchrotron radiation is obvious on comparing Fig. 1(a) with Fig. 1(b). Although the Mo K $\alpha$  map is topographically similar to the synchrotron maps in its broad characteristics, the data are affected far more strongly by noise in the high-order Fourier coefficients, especially near the Pd atom. The synchrotron radiation maps agree well. Both show strong accumulation of electron density around the structural cavity at  $(\frac{1}{2}, \frac{1}{2}, \frac{1}{2})$ , located at the top right-hand corner of the Fig. 1 maps. This feature, though less clearly defined, occurs in both the Mo K $\alpha$  map and in maps based on the data of Takazawa, Ohba & Saito (1988).

Noting that the electron distribution surrounding a relatively heavy atom such as Pd is more difficult to determine accurately, the degree of consistency

between the synchrotron data sets is satisfying. The electron density near Pd is depleted along the Pd—Cl vector. The local minimum occurs 0.5 Å from the Pd nucleus. The electron depletion around the Cl atom has the approximate shape of an isosceles triangle with its apex pointing towards Pd, and its base facing the structural cavity at  $\frac{1}{2}, \frac{1}{2}, 0$  where the density is depleted.



(a)



(b)

Fig. 1.  $\Delta\rho$  for (110) plane of  $K_2PdCl_4$ . (a) Mo  $K\alpha$ , (b) 0.7 Å (1991/92 data). Map borders  $7.0 \times 3.4$  Å; contour intervals  $0.2 e \text{ \AA}^{-3}$ ; positive contours shown by solid lines, zero and negative contours by long and short dashes, respectively.

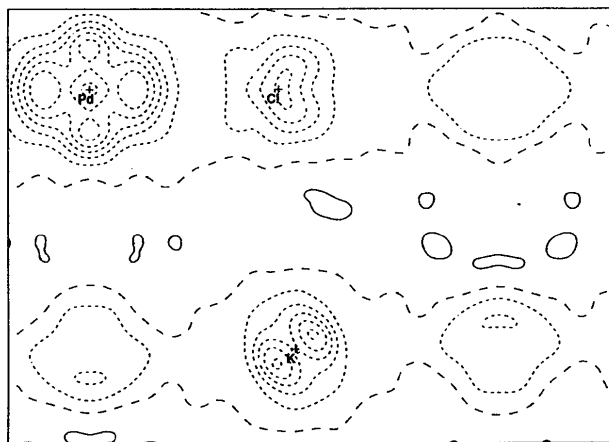


Fig. 2.  $\Delta\rho$  for (111) plane for  $K_2PdCl_4$ , 0.7 Å (1991/92 data). Borders and contours as for Fig. 1.

In general, electron density is removed from the regions where closed inner subshells for each atom overlap with the valence electrons of its neighbours. Density is transferred to regions of low electrostatic potential between the nuclei, except for the regions near structural cavities, where depletion can also occur. These characteristics of the density are broadly consistent with those reported for studies of ideal perovskite structures with synchrotron radiation by Maslen, Spadaccini, Ito, Marumo, Tanaka & Satow (1993). The significant features at the different classes of structural cavity resemble those observed by Maslen & Spadaccini (1989) in the ideal perovskites, where the height of the difference density correlates strongly with the closeness of the packing in the structure. The depletion at  $(\frac{1}{2}, \frac{1}{2}, 0)$  arises from the close packing of atoms in the  $ab$  plane. The accumulation at  $(\frac{1}{2}, \frac{1}{2}, \frac{1}{2})$  results from movement of electrons out of closely packed regions.

Fig. 2 shows the (111) plane for the 0.7 Å data set. The zone of depleted density near the K nucleus has an interesting topography. At the  $-0.2 e \text{ \AA}^{-3}$  level the zone of depleted density extends furthest along the line of the K—Cl vector. Closer to the K nucleus the  $-0.5 e \text{ \AA}^{-3}$  depletion of electron density along the K—Pd vectors is about half as deep as that orthogonally directed towards the structural cavity at  $(\frac{1}{2}, \frac{1}{2}, 0)$ . This topography cannot be explained simply in terms of isotropic  $4s$  functions. States with higher quantum numbers must be involved in the bonding of the K atom in this structure.

The negative K charge is not inconsistent with the local charge depletion around K. The Hirshfeld partitioning process divides the entire deformation density between the constituent atoms, which means that portions of interatomic electron features, including the charge accumulation at  $(\frac{1}{2}, \frac{1}{2}, \frac{1}{2})$ , are assigned to K. When these contributions are combined with the local depletion a net negative charge on K results.

The contributions of computer programs by their authors R. Alden, G. Davenport, R. Doherty, W. Dreissig, H. D. Flack, S. R. Hall, J. R. Holden, A. Imerito, R. Merom, R. Olthof-Hazenkamp, M. A. Spackman, N. Spadaccini and J. M. Stewart to the *Xtal3.0* system (Hall & Stewart, 1990), used extensively in this work, is gratefully acknowledged. The authors also acknowledge the support of the Australian Research Council and of the Japanese Ministry of Education.

#### References

- ALDEN, R., FREER, S. & STEWART, J. (1990). *SCALE1. Xtal3.0 Reference Manual*, edited by S. R. HALL & J. M. STEWART. Univs. of Western Australia, Australia, and Maryland, USA.  
CROMER D. T. & LIBERMAN, D. (1970). *J. Chem. Phys.* **53**, 1891–1898.

- CROMER, D. T. & MANN, J. B. (1968). *Acta Cryst.* **A24**, 321–324.  
 DAVIS, C. L. & MASLEN, E. N. (1978). *Acta Cryst.* **A34**, 743–746.  
 HALL, S. R. & STEWART, J. M. (1990). Editors. *Xtal3.0 Reference Manual*. Univs. of Western Australia, Australia, and Maryland, USA.  
 HIRSHFELD, F. L. (1977). *Isr. J. Chem.* **16**, 198–201.  
 MASLEN, E. N. & SPADACCINI, N. (1989). *Acta Cryst.* **B45**, 45–52.  
 MASLEN, E. N. & SPADACCINI, N. (1993). *Acta Cryst.* **A49**, 661–667.  
 MASLEN, E. N., SPADACCINI, N., ITO, T., MARUMO, F., TANAKA, K. & SATOW, Y. (1993). *Acta Cryst.* **B49**, 632–636.  
 SATOW, Y. & IITAKA, Y. (1989). *Rev. Sci. Instrum.* **60**, 2390–2393.  
 TAKAZAWA, H., OHBA, S. & SAITO, Y. (1988). *Acta Cryst.* **B44**, 580–585.

*Acta Cryst.* (1993). **B49**, 846–852

## Structure and Disorder in Single-Crystal Lead Zirconate, $\text{PbZrO}_3$

BY A. M. GLAZER

*Department of Physics, Clarendon Laboratory, University of Oxford, Parks Road, Oxford OX1 3PU, England*

AND K. ROLEDER AND J. DEC

*Institute of Physics, Silesian University, Uniwersytecka 4, 40-007 Katowice, Poland*

(Received 8 October 1992; accepted 19 May 1993)

### Abstract

The full three-dimensional *single-crystal* crystal structure of the perovskite material  $\text{PbZrO}_3$  ( $M_r = 346.42$ ) has been refined. It is found that the structure is disordered with two substructure components related by a shear of  $c/2$ . Each individual substructure corresponds closely to the tilt system  $a^+ a^- c^0$  of Glazer [*Acta Cryst.* (1972), **B28**, 3384–3392; *Acta Cryst.* (1975), **A31**, 756–762]. The space group was determined to be  $Pbam$  ( $D_{2h}^2$ ) with  $a = 5.889$  (3),  $b = 11.784$  (4) and  $c = 8.226$  (2) Å,  $V = 570.8$  (4) Å<sup>3</sup>,  $Z = 8$ ,  $D_x = 8.06 \text{ Mg m}^{-3}$ ,  $\text{Mo K}\alpha$ ,  $\lambda = 0.71069$  Å,  $\mu = 612.68 \text{ cm}^{-1}$ ,  $T = 297 \text{ K}$ . The structure was refined to  $R = 0.0596$  and  $wR = 0.0753$  for 246 unique reflections, and, apart from the choice of space group, is very similar to that proposed by Whatmore (PhD thesis, Univ. of Cambridge, England, 1976). Comments are made on the relationship between the single-crystal structure of  $\text{PbZrO}_3$  and that determined from polycrystalline samples.

### Introduction

The perovskite compound  $\text{PbZrO}_3$  has been of interest for some time because of the complex nature of its structure and also because it is the end member of the technologically important solid-solution series  $\text{PbZr}_{1-x}\text{Ti}_x\text{O}_3$ . For a long time there has been some controversy in the literature as to whether this material is ferroelectric or antiferroelectric. Roberts (1951) found evidence of piezoelectricity, thus pointing to a non-centrosymmetric space group. However,

to observe this effect Roberts polarized a ceramic disc by applying a d.c. or pulsed electric field while cooling through the phase transition from 523 to 373 K. Given the well known problem of space charges in this material and taking into account the manner in which the sample was polarized, together with the very small effect found, suggests that this piezoelectric effect was probably due to an electret state induced by thermal charging, rather than to the symmetry of the crystal structure. It is not surprising, therefore, that others (*e.g.* Fesenko & Smotrakov, 1976; Scott & Burns, 1972) were unable to find polar effects although the occurrence of complex twinning in their crystals may have made such measurements suspect.

The crystal structure was first proposed by Sawaguchi, Maniwa & Hoshino (1951), who showed from weak X-ray superlattice reflections that the pseudocubic perovskite unit cell was given by  $4\mathbf{a}_p \times 4\mathbf{b}_p \times 2\mathbf{c}_p$ , with  $\mathbf{a}_p = \mathbf{b}_p$ . The quadrupling of the pseudocubic  $\mathbf{a}_p$  and  $\mathbf{b}_p$  axes could be explained by Pb displacements from their prototypic perovskite sites, as shown in Fig. 1. Sawaguchi *et al.* (1951) determined that the displacements were approximately 0.2 Å, and that the true space group was either  $Pbam$  or  $Pba2$  with cell dimensions  $\mathbf{a}_o = 5.87$ ,  $\mathbf{b}_o = 11.74$  and  $\mathbf{c}_o = 8.20$  Å. They were unable to locate the positions of the Zr or O ions, or to detect any displacements of the Pb ions out of the  $(001)_o$  planes. Jona, Shirane, Mazzi & Pepinsky (1957) made a more detailed study of the structure using a combination of X-ray single-crystal and neutron powder diffraction. They found that the space